J Biol Inorg Chem (2006) 11:791–801
DOI 10.1007/s00775-006-0122-9

ORIGINAL PAPER

Synthesis, characterization, antitumoral and osteogenic activities of quercetin vanadyl(IV) complexes

Evelina G. Ferrer · María V. Salinas · María J. Correa · Luciana Naso · Daniel A. Barrio · Susana B. Etcheverry · Luis Lezama · Teófilo Rojo · Patricia A. M. Williams

Received: 21 December 2005 / Accepted: 31 May 2006 / Published online: 5 July 2006

Abstract The development of new vanadium derivatives with organic ligands, which improve the beneficial actions (insulin-mimetic, antitumoral) and decrease the toxic effects, is of great interest. A good candidate for the generation of a new vanadium compound is the flavonoid quercetin because of its own anticarcinogenic effect. The complex $[VO(Quer)_2EtOH]_n$ (QuerVO) has been synthesized and characterized by means of different spectroscopic techniques (UV–vis, Fourier transform IR, electron paramagnetic resonance) and its magnetic and stability properties. The inhibitory effect on bovine alkaline phosphatase (ALP) activity has been tested for the free ligand, the complex as well as for the vanadyl(IV) (comparative purposes). The biological activity of the complex on the proliferation of two osteoblast-like cells in culture, a normal one (MC3T3E1) and a tumoral one (UMR106), has been compared with that of the vanadyl(IV) cation and quercetin. The differentiation osteoblast markers ALP specific activity and collagen synthesis have been also tested. In addition, the effect of QuerVO on the activation of the extracellular regulated kinase (ERK) pathway is reported. The bone antitumoral effect of quercetin alone was established with the cell proliferation assays (it inhibits the proliferation of the tumoral cells and does not exert any effect on the normal osteoblasts). Moreover, the complex exerts osteogenic effects since it stimulates the type I collagen production and is a weak inhibitory agent upon ALP activity. Finally, QuerVO stimulated the ERK phosphorylation in a dose–response manner and this activation seems to be involved as one of the possible mechanisms for the biological effects of the complex.

Keywords Vanadium · Quercetin · Antitumoral effects · Osteogenic effects · Osteoblasts

D. A. Barrio · S. B. Etcheverry
Cátedra de Bioquímica Patológica, Facultad de Ciencias Exactas, Universidad Nacional de La Plata, 47 y 115, 1900 La Plata, Argentina

L. Lezama · T. Rojo
Departamento de Química Inorgánica, Facultad de Ciencia y Tecnología, Universidad del País Vasco, Apdo 644, 48080 Bilbao, Spain

E. G. Ferrer · M. V. Salinas · M. J. Correa · L. Naso · S. B. Etcheverry · P. A. M. Williams (✉)
CEQUINOR (Centro de Química Inorgánica), Facultad de Ciencias Exactas, Universidad Nacional de La Plata, 47 y 115, 1900 La Plata, Argentina
e-mail: williams@quimica.unlp.edu.ar

Introduction

Flavonoids, 2-phenyl-benzo-α-pyrones are nonnutritive polyphenolic compounds of plants that have recently aroused considerable interest owing to their broad pharmacological activity. Quercetin, 3′,3, 4′,5,7-pentahydroxyflavone (Fig. 1), belongs to a large group of naturally occurring flavonoid compounds found in plants, foods and beverages, and is a major dietary flavonoid [1]. Besides, flavonoids represent a subgroup of intensely colored polyphenolic phytochemicals. They contribute to plant color, providing a spectrum of colors from red to blue in flowers, fruit and leaves. Owing to some interesting health-benefiting properties, flavonoids have been widely examined with respect to their chemistry and biological activity. They are acknowledged to be antioxidants and radical

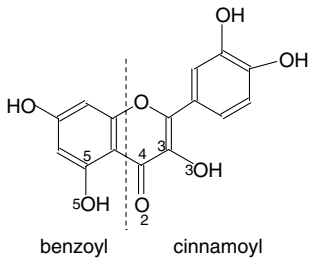

Fig. 1 Schematic structure of quercetin

scavengers. Beneficial effects of flavonoids on human health have gained increasing interest during the last few years owing to their antitumoral and antibacterial activities [2–9].

Flavonoids can also act as metal chelators [3, 10–12]. Their ability to form complexes with some *p*-, *d*- and *f*-electron metals makes them interesting analytical reagents. Quercetin possesses three possible chelating sites in competition: the 3-hydroxychromone, the 5-hydroxychromone and the 3′,4′-dihydroxyl groups and is most widely used for detection of metals bound to flavonoid ligands owing to their highly sensitive molecular fluorescence properties. Analytical procedures have been developed for Al, Cr, W, Zr, Ti, Fe, Mo, Zr, Hf, Ge, Ru, Pd, Os, Pt and Au [13].

Vanadium is an important trace element for different organisms. The coordination chemistry of vanadium has been receiving increasing interest since it was found to be beneficial in various biological systems [14, 15]. One of the results of the intensive investigations of vanadium has been the discovery that vanadium compounds in various oxidation states have insulin-mimetic and anticarcinogenic properties [16]. Its physiological effects in many cases stem from the good complexation behavior of VO^{2+}, and the chemical similarity between phosphate, vanadate and pentacoordinated vanadyl(IV) complexes. Because of the low toxicity of VO(IV), a large number of its complexes have been isolated, characterized and tested for biological activity [17, 18].

Studies of the interaction between quercetin and its vanadyl complex with UMR106 tumoral cells are important to further understand the pharmacology of quercetin. We describe here the synthesis and characterization of a new quercetin complex with vanadyl(IV) cation and the biological effects of this complex and the free ligand upon the inhibition on bovine intestinal alkaline phosphatase (ALP) and on the proliferation (on normal and tumoral osteoblasts), differentiation (ALP specific activity and collagen synthesis on osteosarcoma cell lines) and the signal transduction pathways involved in the mechanism of action of $[VO(Quer)_2EtOH]_n$ (QuerVO) through its effect on the activation of extracellular regulated kinases (ERKs).

Most of the cells in multicellular organisms and in culture systems are surrounded by a complex mixture of nonliving material that makes up the extracellular matrix (ECM). In vertebrates, the ECM is made by carbohydrates and proteins plus minerals in the case of bone. In bone tissue the ECM is secreted by osteoblasts. It consists of protein fiber embedded in an amorphous mixture of huge protein–polysaccharide (‘‘proteoglycan’’) molecules. Collagen is the most important protein component of the ECM and it is essential for the mineralization process. Its synthesis increases as the preosteoblasts turn to mature osteoblasts [19]. As hard tissue is the main storage site for vanadium in vertebrates, it is of great interest to investigate the effect of vanadium derivatives on the differentiation of bone-related cells in culture. Differentiation is a complex physiological process and for osteoblasts there are some important markers of cellular differentiation, such as the specific activity of the ALP and the synthesis of collagen for the ECM formation. For the aforementioned reasons, the osteogenic activities of quercetin and the complex in osteoblastic UMR106 cells (which express a high level of ALP and collagen) have been tested. Besides, the potential antitumoral effect of the ligand and the vanadyl(IV) complex in bone-related cells has been investigated in the tumoral osteoblast cell line (UMR106) and compared with the normal MC3T3E1 osteoblasts in culture. In an earlier report another quercetin VO(IV) complex was reported and its insulin-mimetic properties were also studied. This complex was obtained under different experimental conditions and it has different physicochemical properties [20].

The results show that quercetin may act as an antitumoral agent owing to its inhibitory effect upon tumoral cell proliferation (the ligand does not affect the proliferation of the nontransformed osteoblasts). Besides, the complex plays an important role as an osteogenic agent, promoting collagen synthesis at low doses.

Materials and methods

Quercetin dihydrate (Sigma) and $VOCl_2$ (50% solution, Carlo Erba) were used as supplied. Corning or Falcon provided tissue culture materials. Dulbecco’s modified Eagle’s medium (DMEM), and trypsin–EDTA were purchased from Gibco (Gaithersburg,

MD, USA) and fetal bovine serum (FBS) was from GibcoBRL (Life Technologies, Germany). All other chemicals used were of analytical grade. The Electronic UV–vis spectra were recorded with a Hewlett-Packard 8453 diode-array spectrophotometer. IR spectra were recorded with a Bruker IFS 66 Fourier transform IR spectrophotometer from 4,000 to 400 cm^{-1} using the KBr pellet technique. A Bruker ESP300 spectrometer operating at X-band and equipped with standard Oxford Instruments low-temperature devices (ESR900/ITC4) was used to record the spectra of the compounds at different temperatures. The magnetic field was measured with a Bruker BNM 200 gaussmeter, and the frequency inside the cavity (rectangular ER4102ST) was determined by using a Hewlett-Packard 5352B microwave frequency counter. Anisotropic X-band electron paramagnetic resonance (EPR) spectra of frozen solutions were recorded at 140 K, after addition of 5% of dimethyl sulfoxide to ensure good glass formation. A computer simulation of the EPR spectra was performed using the program SimFonia (WIN-EPR SimFonia version 1.25, Bruker Analytische Messtecnik, 1996). Magnetic susceptibility measurements on polycrystalline samples were performed in the temperature range 5–300 K with a Quantum Design MPMS-7 superconducting quantum interference device magnetometer and using an applied field of 0.1 T. Diamagnetic corrections of the constituent atoms were estimated from Pascal's constants. Elemental analysis for carbon and hydrogen was performed using a Carlo Erba EA 1108 analyzer. Vanadium content was determined by the tungstophosphovanadic method [21].

Synthesis of $[VO(Quer)_2EtOH]_n$

A 50% aqueous solution of $VOCl_2$ (0.5 mmol) was slowly added to a 30 ml ethanolic solution of quercetin (1 mmol) to afford a green solution. After refluxing for 3 h, and maintaining the pH at 4, a green solid was formed. The hot resulting suspension was filtered, washed three times with cold ethanol and air-dried. Anal. Calcd. for $C_{32}H_{24}O_{16}V$: C, 53.71; H, 3.36; V, 7.13. Exp.: C, 53.70; H, 3.30; V, 7.09%. UV–vis spectrum for VO/Quer 0.5/1, methanol: 580 (57.6); 650 (sh) (53.6); 782 (64) nm.

Spectrophotometric titrations

The stoichiometry of the complex was determined by the molar ratio method. A methanolic solution of quercetin (4×10^{-5} M) was prepared and its electronic spectrum recorded. The absorption spectra of different methanolic solutions of 4×10^{-5} M quercetin and $VOCl_2$ in ligand-to-metal ratios from 2 to 0.1 (pH 4) were measured.

Stability studies

The rates of the decomposition reaction of the complex were determined by measuring the variation of the UV–vis spectra with time. The electronic absorption bands had been monitored at 580 nm at 310 K. The compounds were sparingly soluble in water. The dissolution of the complexes (14 and 20 mM) was performed in ethanol or methanol, respectively. In order to prevent contact of the sample with atmospheric oxygen, the measurements were carried out directly in the cell of the spectrophotometer, with the corresponding stoppers and Parafilm.

ALP assays

The effect of quercetin, and QuerVO on bovine intestinal ALP activity was determined spectrophotometrically, and compared with data of vanadyl(IV) cation. The solutions of the free ligand and the complex were prepared by dissolving each solid in methanol and diluting with the incubation buffer solution. At the maximum concentrations, about 1% of methanol is present. The reaction was started by the addition of the substrate (*p*-nitrophenylphosphate, *p*-NPP), and the generation of *p*-nitrophenol (*p*-NP) was monitored by the absorbance changes at 405 nm. Briefly, the experimental conditions for ALP specific activity measurement were as follows: 1 μg ml^{-1} bovine intestinal ALP and 5 mM *p*-NPP were dissolved in the incubation buffer (55 mM glycine and 0.55 mM $MgCl_2$, pH 10.5) and held for 10 min. The effects of the compounds were determined by addition of different concentrations (10–100 μmol l^{-1}) of each one to the preincubated mixtures. The effect of each concentration was tested at least in triplicate in three different experiments. Basal conditions, in the absence of any compound, were determined as the absorbance of *p*-NPP hydrolysis at 310 K and pH 10.5. The enzymatic reaction rates inhibited by quercetin and its vanadium complex were determined like in the basal conditions but in the presence of the different concentrations of each of the systems investigated. Data were expressed as the mean ± the standard error of the mean (SEM). Statistical differences were analyzed by Student's *t* test.

Cell culture

Rat osteosarcoma UMR106 and osteoblastic non-transformed mouse calvaria derived MC3T3E1 cells were grown in DMEM supplemented with 10% (V/V) FBS and antibiotics (100 U ml^{-1} penicillin and 100 μg ml^{-1} streptomycin) in a humidified atmosphere of 95% air/5% CO_2. Cells were grown at a 50–60% confluence and were subcultured using 0.1% trypsin–1 mM EDTA in a Ca^{2+}–Mg^{2+}-free phosphate buffered saline (PBS). For experiments, about 5.2×10^4 cells per well (UMR106) and 4.0×10^4 cells per well (MC3T3E1) were plated into 24-wellsplates. After the culture reached 70% confluence, the cells were washed twice with DMEM. The cells were incubated in 0.5 ml DMEM overnight with the vanadium compound and quercetin at different doses in serum-free DMEM.

Cell proliferation assay

For the mitogenic bioassay, the method described by Okajima et al. [22] was used with some modifications. The cells in 24-well plates were washed with PBS and fixed with 5% glutaraldehyde/PBS at room temperature for 10 min. The cells were then stained with 0.5% crystal violet/25% methanol for 10 min and the dye solution was discarded. After that, the plate was washed with water and dried. The crystal violet fixed by the cells was quantified at 540 nm after an extraction procedure. The dye in the cells was extracted using 0.5 ml per well 0.1 M glycine/HCl buffer, pH 3.0 with 30% methanol and transferred to test tubes. The correlation between cell number per well and the absorbance at 540 nm of the diluted extraction sample after crystal violet staining has previously been established [23]. Data were expressed as the mean ± SEM. Statistical differences were analyzed using Student's *t* test. *t* tests were done to compare treated and untreated cultures. Fresh solutions of the vanadyl(IV) complex were added to the culture dishes. The studies were performed in the range of vanadium concentration of 2.5–100 μmol l^{-1} . Higher concentrations of vanadium compounds proved to be toxic and caused osteoblast death after several hours of incubation [24]. In order to prepare the stock solution for these studies, the complex was dissolved in ethanol, and different aliquots were diluted in the culture medium, and added to the cells. This procedure takes at least 5 min. The effect of ethanolic solutions on the cells was checked. The results showed that the maximum ethanol concentration used in the wells of the culture did not produce any damage to the osteoblasts.

Cell differentiation assays

ALP specific activity

The ALP specific activity has been used as a marker of osteoblast phenotype [21, 25, 26]. Cells were grown in 24-well plates until 90–100% confluence, and the monolayers were washed twice with serum-free DMEM. Then the cells were incubated overnight with serum-free DMEM and different doses of QuerVO (2.5–100 μM) were added. The cell layer was then washed with PBS and solubilized in 0.5 ml 0.1% Triton X-100. Aliquots of the total cell extract (10–20%) were used for protein determination by the Bradford technique [27]. Measurement of ALP activity was carried out by spectrophotometric determination of initial rates of hydrolysis of *p*-NPP to *p*-NP at 310 K for 10 min. The reaction mixture consisted of 10 μl cell extract in 800 μl glycine buffer (55 mM glycine, 0.55 mM $MgCl_2$, pH 10.5). The reaction was initiated by the addition of 100 μl of substrate solution to 5 mM *p*-NPP in glycine buffer. The production of *p*-NP was determined by the absorbance at 405 nm. Under these experimental conditions, the product formation was linear for 15 min.

Collagen production

The synthesis of type I collagen is also a marker of osteoblastic phenotype. The effects of QuerVO, quercetin and VO on this parameter were analyzed by a histochemical method adapted to determine the collagen produced by osteoblasts in culture [28]. UMR106 cells were cultivated on multiwell plates. When the cells reached 90% confluence, the layers were washed three times with PBS and fixed for 1 h with 1 ml of fixation solution (15 ml picric acid solution/5 ml 35% formaldehyde/1 ml glacial acetic acid). After that, the monolayers were washed for 15 min with distilled water with mild agitation and then were colored with 1 ml of dye solution (100 mg Sirius Red in 100 ml of a saturated solution of picric acid) for 1 h with mild agitation. Then, they were washed with 0.01 N HCl to remove the excess of Sirius Red. The dye fixed to the collagen was extracted with 1 ml 0.1 N NaOH with mild agitation for 30 min. Then, the absorbance of the samples was recorded at 550 nm. The content of collagen produced by the cells was obtained by the calibration curve obtained in the same conditions as those reported previously [28].

Western blotting of cell lysates

UMR106 osteosarcoma cells were subcultured into 12-well plates in DMEM supplemented with 100 U ml^{-1} penicillin, 100 μg ml^{-1} streptomycin and 10% (v/v) FBS at 310 K, 5% CO_2. When 100% confluence was reached, the medium was removed and the cells were washed twice with serum-free DMEM. Cells were incubated in serum-free DMEM without the addition of the complex (basal) or with different concentrations of QuerVO, for 1 h. The cells were washed twice with cold PBS and lysed in Laemmli buffer [29]. Protein content was determined in each lysated cellular fractions. Aliquots with equal amounts of protein were separated on 12.5% sodium dodecyl sulfate polyacrylamide gel electrophoresis under reducing conditions. Then, they were transferred to acetate cellulose membranes, and examined by immunoblotting with specific antibodies against the phosphorylated (1:3,000) and nonphosphorylated (1:1,000) ERKs and were revealed by a commercial electrochemical luminescence (ECL) kit.

Results and discussion

Spectrophotometric titrations

Quercetin exhibits a strong absorption band (band I) at 372 nm in methanolic solutions in the UV–vis spectrum. For the determination of the stoichiometry of the VO/quercetin system, spectrophotometric titrations were performed. Following the spectral changes associated with the amount of VO(IV) added, we can see that the absorption band at 370 nm decreases, while a band centered at 432 nm increases (Fig. 2).

The isosbestic point, located at 392 nm, is indicative of the presence of one complex species formed. In the molar ratio plot (Fig. 2, inset) the inflection at the metal-to-ligand ratio of 0.5 is indicative of the formation of a 1:2 VO–quercetin complex.

From Fig. 2 it can be observed that: (1) band I (related to the cinnamoyl residue) remains in place upon vanadyl addition, but its intensity decreases; (2) band II, related to the benzoyl residue, does not shift, but its intensity is increased with metal addition; (3) the new band located at 432 nm corresponds to the M-3-OH-group of quercetin that generates an electronic redistribution between the ligand and the metal, forming a big extended π-bonding system. The electronic transition nπ* of quercetin changes to π–π* with lower energy, favoring the development of a new band at higher wavelength (redshift) [7].

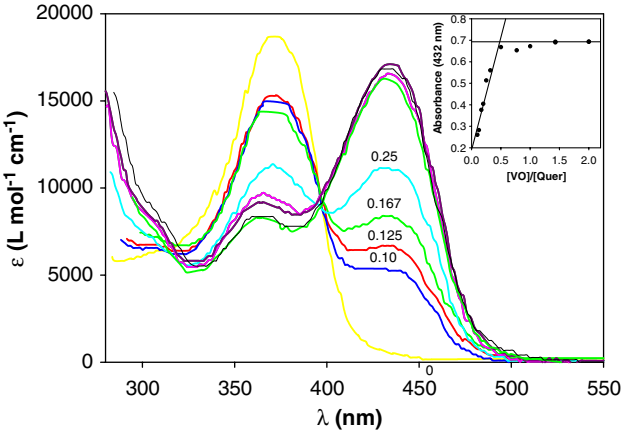

Fig. 2 Spectrophotometric titration spectra of quercetin in methanol (4×10^{-5} M, 0): increasing concentrations of VO(IV) (from 4×10^{-6} mol l^{-1}, 0.10 to 8×10^{-5} mol l^{-1}), pH 4. *Inset*: Molar ratio plot of the spectrophotometric titration of quercetin with VO(IV) at $\lambda = 432$ nm

Vibrational spectra

The main bands and tentative assignments are shown in Table 1.

Evaluating the spectra of the free ligand and the complexes, we can obtain the following information:

- The characteristic stretching ν(C = O) decreases by approximately 30 cm^{-1}. It can be suggested that the VO(IV) coordination occurs through the O carbonyl atom and the 3-OH or 5-OH groups of the ligand after deprotonation [3–6]. The increase in bond order C4 = O2 connected with the increase in C3–O3 in the complex may give rise to a coupling of the vibrations of these two bonds. The new bands at approximately 1,500 and 1,430 cm^{-1} can be considered as associated with the antisymmetric and symmetric stretching modes, respectively, of the C–O group at the chelating site.
- The band related to the ν(C–O–C) mode at 1,264 cm^{-1} is slightly shifted by complex formation, indicating a weak alteration of the ring structure

Table 1 Assignment of the IR spectra of quercetin and $[VO(Quer)_2EtOH]_n$ (*QuerVO*) (band positions in cm^{-1})

	Quercetin	QuerVO
ν(C = O)	1,666 s	1,635 vs
ν_{ring}(C = C)	1,610 vs, 1,562 s	1,602 vs
$\nu(C–O)_{as}$		1,511 m
$\nu(C–O)_s$		1,435 s
ν(C–OH)	1,381 s	1,362 m
ν(C–O–C)	1,264 s	1,280 vs
ν(V = O)		977 m
ν(V–O)		423 w

vs very strong, *s* strong, *m* medium, *w* weak, *vw* very weak

and the lack of interaction of the O ring atom with the metal.

- The bands of the ring at 1,610 and 1,562 cm^{-1} are rather changed by chelation, suggesting some modification in the structure of the two rings.
- The position of the V = O stretching bands is typical for oxygenated spheres around the vanadium centers [30].

EPR and magnetic data

The X-band EPR powder spectrum of the QuerVO complex, recorded at room temperature, is shown in Fig. 3, spectrum A. The main feature is a broad, quasi-isotropic signal, centered about 3,500 G, originating from mutual interactions between neighboring $V^{IV}O$ sites. This type of signal is characteristic of magnetically extended systems of vanadyl(IV) [31]. Some weaker signals are also observed superposed on the central line; they correspond to the hyperfine structure of a V(IV) isolated species (100% abundant ^{51}V nucleus with $I = 7/2$) and must originate from the presence of a small amount of monomeric impurities.

The spin Hamiltonian parameters of the main contribution were estimated by comparison of the room-temperature spectrum with those generated by a computer simulation program working at the second order of perturbation theory (Fig. 3, spectrum B). The calculated values of $g_{\|} = 1.96$ and $g_{\perp} = 1.98$ ($g_{iso} = 1.97$) are in accord with a nearly axial or pseudoaxial ligand field, as is usually observed for vanadium complexes owing to the strong vanadium–oxygen interaction in the vanadyl unit [32].

In order to establish the binding mode of the ligand, frozen-glass EPR studies on dissolved powder were performed ($[VO^{2+}] = 1 \times 10^{-5}$ mol l^{-1}). The spectra obtained display the typical eight-line pattern spectrum for axial-V(IV) systems and indicate the formation of a single species of the complex after its dissolution (Fig. 4). At pH 4, the observed signal originates from a V chromophore with $g_{\|} = 1.940$, $g_{\perp} = 1.979$, $A_{\|} = 174 \times 10^{-4}$ cm^{-1} and $A_{\perp} = 64 \times 10^{-4}$ cm^{-1} ($g_{iso} = 1.966$, $A_{iso} = 101 \times 10^{-4}$ cm^{-1}), very close to those of the VO(IV)-maltol and related systems [33–40]. Small, but significant, changes in the spectra are detected when the pH of the solution was modified (by adding 1 M NaOH solution). At pH 7 the EPR parameters are $g_{\|} = 1.940$, $g_{\perp} = 1.979$, $A_{\|} = 168 \times 10^{-4}$ cm^{-1} and $A_{\perp} = 60 \times 10^{-4}$ cm^{-1} ($g_{iso} = 1.966$, $A_{iso} = 96 \times 10^{-4}$ cm^{-1}), suggesting the formation of a new compound with some modification of the equatorial coordinated groups.

It is known that the parallel component of the hyperfine coupling constant is sensitive to the type of donor atoms on the equatorial positions of the coordination sphere. In this sense, the following empirical relationship is frequently used in order to determine, to a first approximation, the identity of the equatorial ligands in V(IV) complexes:

$$A_z = \sum n_i A_{z,i},$$

where n_i the number of equatorial ligands of type i and $A_{z,i}$ is the contribution to the parallel hyperfine

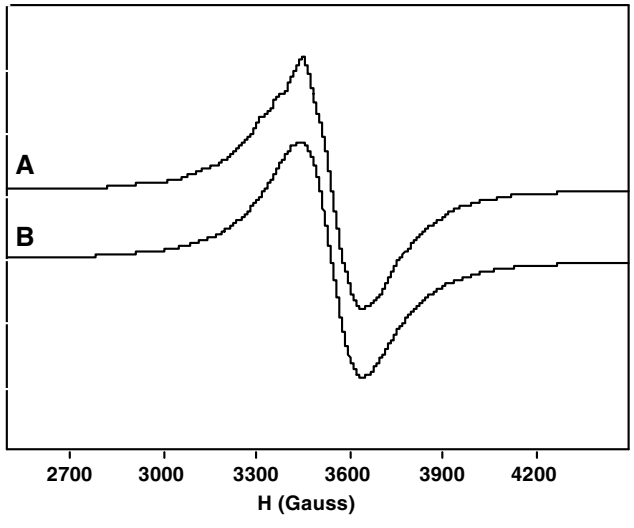

Fig. 3 Experimental (*A*) and calculated (*B*) room-temperature powder electron paramagnetic resonance (*EPR*) spectrum of the $[VO(Quer)_2EtOH]_n$ (*QuerVO*) complex measured at X-band (9.79 GHz)

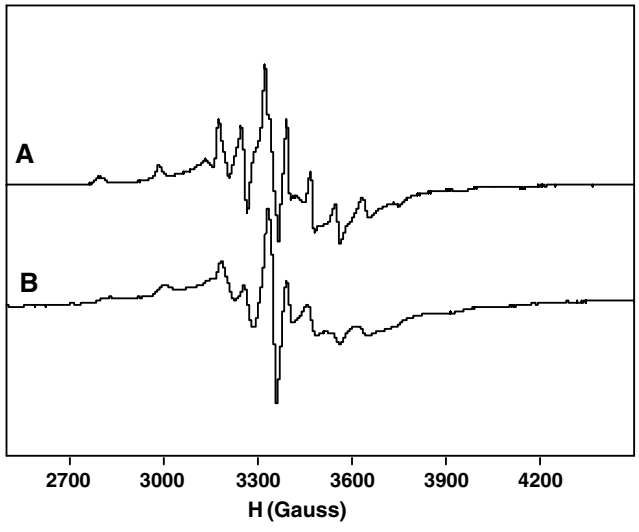

Fig. 4 X-band (9.43 GHz) EPR spectra of aqueous solutions of QuerVO at pH 4 (*A*) and pH 7 (*B*) measured at 140 K

coupling from each of them [32]. Besides, the comparison between the calculated and experimental values of A_z has been used to argue for the presence of specific ligands. For the title compound, the spin Hamiltonian parameters obtained are in the range usually found for O_4 coordination complexes of the vanadyl ion. Moreover, comparable values are predicted by the previous equation considering other complexes with similar donor sets [33–40], and the calculated parameters fit well in the corresponding $g_\parallel$ versus $A_\parallel$ diagram [40, 41]. Considering the contributions to the parallel hyperfine coupling constant of the different coordination modes (CO = 44.7×10^{-4} [42], H_2O = 45.7×10^{-4}, ArO^- = 38.6×10^{-4} and OH^- = 38.7×10^{-4} cm^{-1} [43]), the reduction of $A_\parallel$ with increasing pH (from 174×10^{-4} to 168×10^{-4} cm^{-1}) is due to the incorporation of OH^- ligands in the coordination sphere. This result is in good agreement with the presence at low pH of a *cis*-$VOL_2(H_2O)$ complex and its transformation to $[VOL_2(OH)]^-$ as the pH increases [44].

Magnetic susceptibility measurements of QuerVO were performed between 5 and 300 K. Figure 5 shows the thermal evolution of the reciprocal molar susceptibility, together with a plot of ($\chi_m T$=μ_{eff}^2/8). Over the entire temperature range, the $\chi_m T$ versus T data were well described by a Curie–Weiss law (χ_m=C_m/T–θ), with C_m = 0.36 $cm^3 K\ mol^{-1}$ and θ = –1.6 K. The observed Curie constant agrees quite well with that calculated from the g value (0.365 cm^3 K mol^{-1}). The negative θ value, as well as the overall appearance of the $\chi_m T$ versus T curve are indicative of the presence of antiferromagnetic interactions in this compound [45].

Despite the spin topology involved in the solid being unknown, we tried to fit the magnetic data under different hypotheses: 1D, 2D and 3D regular systems of

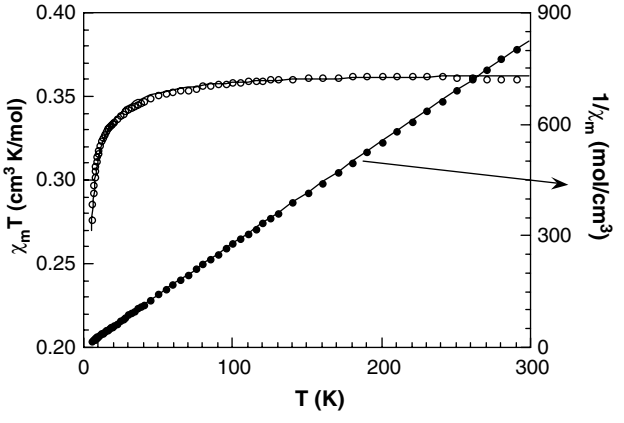

Fig. 5 Temperature dependence of the magnetic susceptibility and the $\chi_m T$ product of QuerVO

S = 1/2. The hypothesis of a dinuclear species in the solid state was discarded considering that (1) the ΔM_s = 2 forbidden transition was not observed and (2) no hyperfine lines corresponding to dimeric species were observed. Finally, the best results were obtained using the Heisenberg model with exchange interaction between pairs of V(IV) ions with spins S_i and S_j of the form:

$$H = \sum_{i>j} H_{ij} = \sum_{i>j} -2J_{ij}S_iS_j,$$

where we assume interactions between nearest-neighbor vanadium ions on a chain (i.e., J_{ij} = J for $j = i\pm1$ and J_{ij} = 0 otherwise).

The temperature dependence of the magnetic susceptibility for the QuerVO complex can be fitted satisfactorily to the empirical function introduced by Hall [46] to represent the numerical calculations performed by Bonner and Fisher [47] describing a uniformly spaced chain of spins with S = 1/2:

$$\chi = \frac{Ng^2\beta^2}{kT}\left(\frac{A + Bx + Cx^2}{1 + Dx + Ex^2 + Fx^3}\right),$$

where $x = |J|/kT$, N and k are the Avogadro and Boltzmann constants, β is the Bohr magneton, A = 0.250, B = 0.14995, C = 0.30094, D = 1.9862, E = 0.68854 and F = 6.0626. The best least-squares fit (solid line in Fig. 5) is obtained with J/k = –1.3 K (J = –0.9 cm^{-1}) and g = 1.97. The agreement factor, defined as SE = $[\Phi/(n - K)]^{1/2}$, where n is the number of data points (65), K the number of adjustable parameters (2) and Φ the sum of squares of the residuals, is equal to 1.4×10^{-5}. The good agreement between experimental and calculated data supports the proposed structural model and the calculated g value is consistent with the EPR results. The weakness of the observed antiferromagnetic coupling is in accordance with an exchange pathway involving hydrogen bonds between adjacent units.

Determination of the stability of the complex

The stability of the complex was evaluated in ethanolic and methanolic solutions at 310 K, in similar conditions to those of the biological studies. Methanol was used in the ALP inhibition determinations, but owing to its toxicity this solvent was replaced by ethanol for the cellular studies. The kinetics of the decomposition of the complex was determined by measuring the variation of the UV–vis spectra with time. The $b_2 \rightarrow e$ electronic absorption bands were monitored at 310 K. Plots of $\ln A(t)$ versus t were linear at least for a half

reaction period and were first order in the concentration of the complex. The value of the rate constant for the decomposition of a 20 mM QuerVO solution in methanol at 310 K was $k = 1.19 \times 10^{-3}$ min^{-1}. On the other hand, in ethanol at 310 K the k value was 7.16×10^{-3} min^{-1} (14 mM QuerVO). Under these conditions the complex was more stable in methanol than in ethanol. These results demonstrated that during the manipulation time of the samples either for ALP inhibition (methanolic solutions) or cellular determinations (ethanolic solutions), a significant amount of the complex is not decomposed (99.4 and 96.5%, respectively).

Biological studies

Bovine intestinal ALP activity

ALP (E.C.3.1.3.1) is a metalloenzyme that catalyzes the hydrolysis of phosphate monoesters. The most widely characterized is an 80,000 molecular weight enzyme from *Escherichia coli*, for which a low-resolution X-ray crystal structure is available [48]. Its dimeric structure contains three nonequivalent metal-binding sites in each subunit. Two of them are occupied by zinc ions, one exerts a catalytic role and the other one has a structural function. The third metal is a Mg(II) cation, also playing a structural role.

In Fig. 6 the effects of the oxovanadium(IV) complex and the free ligand on the ALP activity are shown. The effect of VO(IV) is also displayed. As can be seen, the inhibition exerted by quercetin takes place at concentrations higher than 50 μmol l^{-1}, whereas its vanadyl(IV) complex is inhibitory over the whole range of concentrations tested in a dose–response manner. At concentrations of 100 μmol^{-1}, the complex produces a greater inhibition of the ALP activity than the free ligand (approximately 20 vs. ca. 5%, respectively).

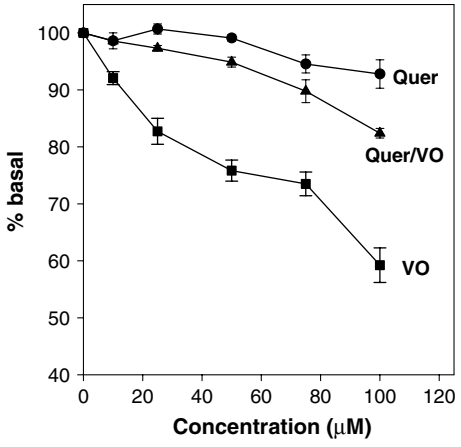

Fig. 6 Effect of quercetin, QuerVO and VO(IV) on alkaline phosphatase activity from bovine intestinal mucose. The initial rate was determined by incubation of the enzyme at 310 K for 10 min in the absence or presence of variable concentrations of the inhibitors. The values are expressed as the mean ± the standard error of the mean (*SEM*) ($n = 9$)

The inhibitory effect of vanadium compounds on the activity of the enzymes that catalyze phosphoryl group transference may be attributed to the formation of a trigonal bipyramidal transition state analog [49]. These phosphorous-mimicking vanadium compounds, with a structure closer to the transition state than that of the phosphorous compound, likely fit more tightly in the active site, causing inhibition of the enzymatic reaction [48]. Although the trigonal bipyramidal coordination geometry is usual for vanadium(V) but not for the vanadyl(IV) cation, it has recently been demonstrated that this coordination structure can be attained by VO^{2+} in the presence of flexible ligands such as proteins and enzymes [50, 51].

The results obtained with the flavonoid–VO complex validate the fact that complexes having a hard donor set of ligands that form particularly strong complexes with the vanadyl cation (C = O$^-$ and O$^-$, in this case) [52, 53] better adopt the transition state structure of ALP, being in this way inhibitors of the enzyme.

Cell proliferation

The results of the effects of the complex, the free ligand and the inorganic vanadyl(IV) cation on osteoblast proliferation can be observed in Fig. 7. According to these results the free ligand quercetin showed potential antitumoral properties since it inhibited the proliferation of UMR106 tumoral cells, while practically it did not cause any effect on the proliferation of the nontransformed osteoblasts. The proliferative behavior of the free ligand was modified upon coordination to the metal center. The QuerVO complex displayed biphasic behavior with a slight stimulation of the proliferation of both cell lines in the low range of concentrations and was an inhibitory agent at higher doses. The complex was more cytotoxic towards normal osteoblasts. Figure 7 also shows the effect of the free vanadyl(IV) cation of both cell lines, which was in agreement with previously reported results [23, 54].

Cell differentiation

To evaluate the effects of vanadium derivatives on cell differentiation, their action on ALP specific activity and

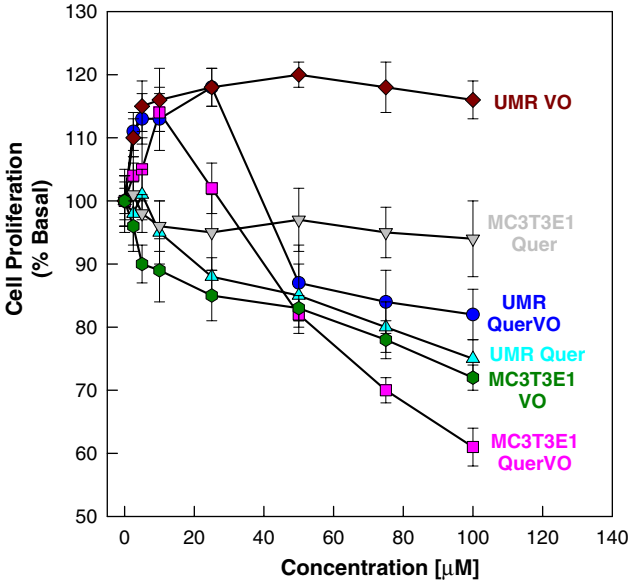

Fig. 7 Effect of QuerVO, VO and quercetin on UMR106 and MC3T3E1 osteoblast-like cell proliferation. Cells were incubated in serum-free Dulbecco's modified Eagle's medium (*DMEM*) alone (basal) or with different concentrations of the compounds at 310 K for 24 h. The results are expressed as percentage basal and represent the mean ± SEM (n = 9)

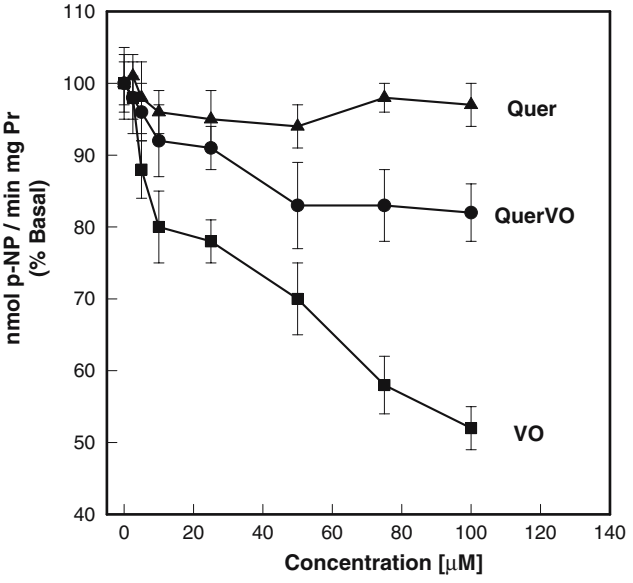

Fig. 8 Effect of QuerVO, quercetin and VO on ALP specific activity. UMR106 cells were incubated either in serum-free DMEM alone (basal) or with different concentrations of the compounds at 310 K for 24 h. Basal activity was 1 μmol *p*-nitrophenol (*p*-NP) per minute per milligram of protein. The results are expressed as percentage basal and represent the mean ± SEM (n = 9)

collagen type I synthesis was investigated in UMR106 cells. Besides the inorganic species of vanadium(IV) and vanadium(V), different VO(IV) cation complexes produced inhibition of the specific enzymatic activity of ALP on osteoblast-like cells in culture [23, 25, 54–59]. Similar behavior has been found with quercetin as the ligand. Nevertheless, the inhibition was lower than that of the free vanadyl(IV) cation. On the other hand, the reduction of the enzyme activity due to the free ligand, quercetin, was very small (Fig. 8). The inhibitory pattern has also been reported for the activity of bovine mucose intestinal ALP [60–63].

In Fig. 9 it can be seen that QuerVO promoted the synthesis of collagen in the range 2.5–10.0 μM, being more efficient than the vanadyl-free cation. Besides, quercetin did not exert any effect on this parameter. These results suggest a stimulatory action on osteoblast differentiation because of the production of one of the most important proteins of the ECM.

Altogether these observations showed that the complexation of quercetin with vanadium improved the potential osteogenic properties of the free parental drugs.

Action of QuerVO on activation of ERKs in UMR106 cells

To investigate the signal transduction pathways involved in the mechanism of action of the QuerVO complex, we examined its effect on the activation of ERK. The action of the complex on the activation of the ERKs was studied by ECL. Proteins in the cell extracts were separated by electrophoresis and exam-

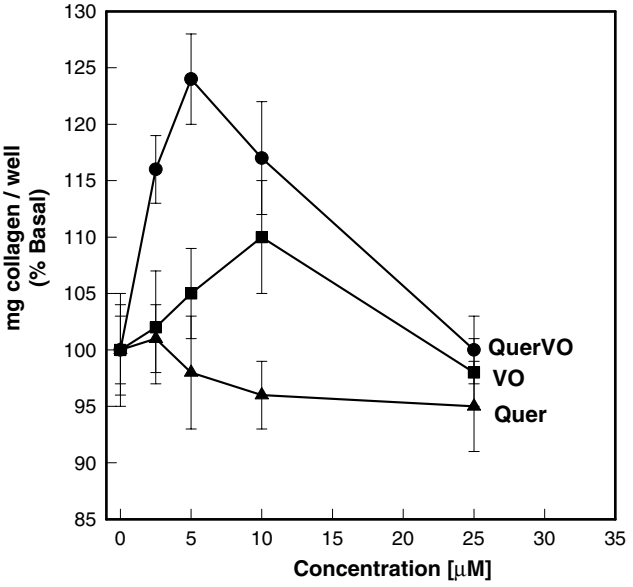

Fig. 9 Synthesis of type I collagen: effects of QuerVO, quercetin and VO on UMR106 cells. The cells were cultivated on multiwell plates up to 100% confluence in the absence (basal) or in the presence of the compounds for 48 h. After fixation, the monolayers were colored with Sirius Red. The absorbance of the samples was recorded at 550 nm. The results are expressed as percentage basal and represent the mean ± SEM (n = 9)

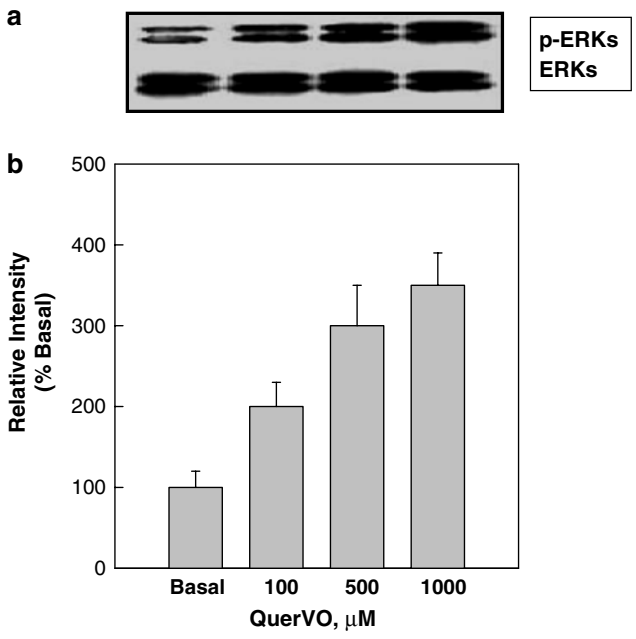

Fig. 10 Western blot (**a**) and dose–response (**b**) of QuerVO-induced extracellular regulated kinase (*ERK*) phosphorylation. Confluent UMR106 cells were treated with different concentrations of QuerVO for 1 h. Cells were lysed and proteins were separated by sodium dodecyl sulfate polyacrylamide gel electrophoresis and transferred to nitrocellulose membrane. For immunoblots, either anti-phosphorylated-ERK or anti-ERK antibodies were used previous stripping. The relative intensities of the stimulation were corrected for total ERK, as determined by densitometry, and are expressed as percentage basal. Similar results were obtained in three independent experiments performed by triplicate

ined by immunoblotting with specific antibodies against the phosphorylated and nonphosphorylated forms of ERK. The results (Fig. 10b) showed that this compound stimulated the phosphorylation of ERKs in a dose–response manner, enhancing their activation. The expression of the nonphosphorylated ERKs was not affected by the complex. A representative immunoblot is shown for ERK and phosphorylated ERK in Fig. 10a. These results point to the fact that QuerVO may be involved through the ERK pathway in the mitogenic effect in osteoblasts in culture.

Conclusions

As part of a research project devoted to developing new vanadium derivatives with interesting biological properties, a new complex of vanadyl(IV) cation with the flavonoid quercetin has been prepared and characterized, both in solution and in the solid state. The complex is formed at pH 4. The compound is very scarcely soluble in water and the solubility increases in methanol or ethanol. Spectrophotometric titration and elemental analysis suggest the formation of a metal-to-ligand 1:2 complex. Using IR spectroscopy, we inferred the coordination to the carbonyl group of the ligand and one of the neighboring deprotonated OH groups. With EPR measurements the axial coordination sphere was established at pH 4 and the deprotonation of the aqua to the hydroxo ligand was detected at pH 7. Magnetic measurements revealed a weak antiferromagnetic coupling with an exchange pathway involving hydrogen bonds between adjacent units. This green quercetin complex differs from the brown compound previously obtained. A possible explanation for this disagreement may be the difference of the solvent system, and the possible differences in the preparation conditions (molar metal-to-ligand ratio and pH values, that were not reported in [20]).

The biological studies suggest that the free ligand quercetin may be a good candidate to be further evaluated in the treatment of bone tissue tumors since its effect has been more deleterious for the tumoral osteoblasts than for the normal cells. On the other hand, the complexation of quercetin with the vanadium center does not improve its potential anticarcinogenic properties. Nevertheless, from the point of view of the cellular differentiation, the QuerVO complex seems to be a promising compound because it stimulates type I collagen production and shows a slight inhibitory effect on ALP specific activity, two markers of osteoblastic differentiation. In fact, the behavior of QuerVO on these parameters points to its potential value for promoting osteoblast differentiation, a crucial stage in the physiology of bone. The activation of ERK pathways seems to be involved at least as one possible mechanism in the biological effects of QuerVO.

Acknowledgments This work was supported by UNLP, CONICET, CICPBA, ANPCyT (PICT 10968) and Eusko Jaularitza/Gobierno Vasco MV-2004-3-39. E.G.F., D.A.B. and S.B.E. are members of the Carrera del Investigador, CONICET. P.A.M.W. is a member of the Carrera del Investigador CICPBA, Argentina.

References

1. Harborne JB, Baxter H (1999) The handbook of natural flavonoids. Wiley, Chichester
2. Rice-Evans CA, Packer L (1998) Flavonoids in health and disease. Dekker, New York
3. Bravo A, Anacona JR (2001) Transition Met Chem 26:20–23
4. Zhou J, Wang L, Wang J, Tang N (2001) Transition Met Chem 26:57–63
5. Zhou J, Wang L, Wang J, Tang N (2001) J Inorg Biochem 83:41–48
6. Cornard JP, Merlín JC (2002) J Inorg Biochem 92:19–27

7. Kang J, Zhuo L, Lu X, Liu H, Zhang M, Wu H (2004) J Inorg Biochem 98:79–86
8. Kanadaswami C, Lee LT, Lee PP, Hwang JJ, Ke FC, Huang YT, Lee MT (2005) In Vivo 5:895–909
9. Kuo SM (1996) Cancer Lett 110:41–48
10. Pusz J, Kopacz M (1992) Pol J Chem 66:1935–1940
11. Escandar GM, Sala LF (1991) Can J Chem 69:1994–2001
12. Le Nest G, Caille O, Woudstra M, Roche S, Burlat B, Belle V, Guigliarelli B, Lexa D (2004) Inorg Chim Acta 357:2027–2037
13. Balcerzak M, Kopacz M, Kosiorek A, Swiecick E, Kus S (2004) Anal Sci 20:1333–1337
14. Chasteen ND (ed) (1990) Vanadium in biological systems. Kluwer, Dordrecht
15. Sigel H, Sigel A (eds) (1995) Metal ions in biological system. Vanadium and its role in life, vol 31. Dekker, New York
16. Orvig C, Thompson KH, Battell M, McNeil JH (1995) In: Sigel H, Sigel A (eds) Metal ions in biological system. Vanadium and its role in life, vol 31. Dekker, New York, pp 575–594
17. Sakurai H, Fujii K, Fujimoto S, Fujisawa Y, Takechi K, Yasui H (1998) In: Tracey AS, Crans DC (eds) Vanadium compounds: chemistry, biochemistry and therapeutic applications. ACS symposium series 711. American Chemical Society, Washington, pp 344–352
18. Thompson KH, Orvig C (2001) Coord Chem Rev 1033:219–221
19. Quarles LD, Yohay DA, Lever LW, Caton R, Wenstrup RJ (1992) J Bone Miner Res 7:683–692
20. Shukla R, Barve V, Padhyeb S, Bhondea R (2004) Bioorg Med Chem Lett 14:4961–4965
21. Onishi M (1988) Photometric determination of traces of metals, part II, 4th edn. Wiley, New York
22. Okajima T, Nakamura K, Zhang H, Ling N, Tanabe T, Yasuda T, Rozenfeld RG (1992) Endocrinology 130:2201–2212
23. Cortizo AM, Etcheverry SB (1995) Mol Cell Biochem 145:97–102
24. Cortizo AM, Bruzzone L, Molinuevo S, Etcheverry SB (2000) Toxicology 147:89–99
25. Etcheverry SB, Crans DC, Keramidas AD, Cortizo AM (1997) Arch Biochem Biophys 338:7–1462
26. Stein GS, Lian JB (1993) Endocr Rev 14:424–442
27. Bradford M (1976) Anal Biochem 72:248–254
28. Tullberg-Reinert H, Jundt G (1999) Histochem Cell Biol 112:271–276
29. Laemmli EK (1970) Nature 227:680–685
30. Allegretti Y, Ferrer EG, González Baró AC, Williams PAM (2000) Polyhedron 19:2613–2619
31. Costa Pessoa J, Tomaz I, Henriques RT (2003) Inorg Chim Acta 356:121–132
32. Chasteen ND (1981) In: Berliner LJ, Reuben J (eds) Biological magnetic resonance, vol 3. Plenum, New York
33. Buglyó P, Kiss E, Fábián I, Kiss T, Sannna D, Garrribba E, Micera G (2000) Inorg Chim Acta 306:174–183
34. Amin SS, Cryer K, Zhang B, Dutta SK, Eaton SS, Anderson OP, Miller SM, Reul BA, Brichard SM, Crans DC (2000) Inorg Chem 39:406–416
35. Chruscinska E, Garriba E, Micera G, Panzanelli A (1999) J Inorg Biochem 75:225–232
36. Hanson GR, Sun Y, Orvig C (1996) Inorg Chem 35:6507–6512
37. Stewart CP, Porte AL (1972) J Chem Soc Dalton Trans 1661–1666
38. Caravan P, Gelmini L, Glover N, Geoffrey Herring F, Li H, McNeill JH, Rettig SJ, Setyawati IA, Shuter E, Sun Y, Tracey AS, Yuen VG, Orvig C (1995) J Am Chem Soc 117:12759–12770
39. Kiss T, Jakush T, Kilyén M, Kiss E, La Katos A (2000) Polyhedron 19:2389–2401
40. Delgado TC, Tomaz AI, Correia I, Costa Pessoa J, Jones JG, Geraldes CFGC, Margarida M, Castro CA (2005) J Inorg Biochem 99:2328–2339
41. McPhail DB, Goodman BA (1987) J Chem Soc Faraday Trans 83:3627–3633
42. Costa Pessoa J, Cavaco I, Correia I, Tomaz I, Duarte T, Matias PM (2000) J Inorg Biochem 80:35–39
43. Cornman CR, Zovinka EP, Boyajian YD, Geiser-Bush KM, Boyle PD, Sing P (1995) Inorg Chem 34:4213–4219
44. Tolis EJ, Teberekidis VI, Praptopoulou C, Terziz A, Sigalas MP, Deligiannakis Y, Kabanos TA (2001) Chem Eur J 7:2698–2710
45. Mabbs FE, Machin DJ (1961) Magnetism and transition metal complexes. Chapman & Hall, London
46. Hall JW (1977) PhD thesis, North Caroline University, cited by Hatfield WH (1981) J Appl Phys 52:1985–1990
47. Bonner JC, Fisher ME (1964) Phys Rev 135:A640–A658
48. Bertini I, Luchinat C (1983) In: Sigel H (ed) Metal ions in biological systems, vol 15. Dekker, New York, pp 101–156
49. Posner BI, Faure R, Burgess JW, Bevan AP, Lachance D, Zhang-Sun G, Fantus IG, Ng JB, Hall DA, Soo Lum B, Shaver A (1994) J Biol Chem 6:4596–4604
50. Garriba E, Micera G, Panzanelli A, Sanna D (2003) Inorg Chem 42:3981–3987
51. Kustin K (1998) In: Tracey AS, Crans DC (eds) Vanadium compounds: chemistry, biochemistry and therapeutic applications. ACS symposium series 711. American Chemical Society, Washington, pp 170–185
52. Grant CV, Geiser-Busch KM, Cornman CR, Britt RD (1999) Inorg Chem 38:6285–6288
53. Ferrer EG, Salinas MV, Correa MJ, Vrdoljak F, Williams PAM (2005) Z Naturforsch 60b:305–311
54. Etcheverry SB, Williams PAM, Barrio DA, Sálice VC, Ferrer EG, Cortizo AM (2000) J Inorg Biochem 80:169–171
55. Barrio DA, Williams PAM, Cortizo AM, Etcheverry SB (2003) J Biol Inorg Chem 8:459–468
56. Williams PAM, Barrio DA, Etcheverry SB (2004) J Inorg Biochem 98:333–342
57. Molinuevo MS, Barrio DA, Cortizo AM, Etcheverry SB (2004) Cancer Chemother Pharmacol 53:163–172
58. Etcheverry SB, Barrio DA, Zinczuk J, Williams PAM, Baran EJ (2005) J Inorg Biochem 99:2322–2327
59. Williams PAM, Etcheverry SB, Barrio DA, Baran EJ (2006) Carbohydr Res 341:717–724
60. Crans DC, Bunch RL, Theisen LA (1989) J Am Chem Soc 111:7597–7607
61. Cortizo AM, Sálice VC, Etcheverry SB (1994) Biol Trace Elem Res 41:331–339
62. Williams PAM, Barrio DA, Etcheverry SB (1999) J Inorg Biochem 75:99–104
63. Etcheverry SB, Barrio DA, Williams PAM, Baran EJ (2001) Biol Trace Elem Res 84:227–237